



Aalborg Universitet

AALBORG UNIVERSITY  
DENMARK

## Impact of Wind Shear and Tower Shadow Effects on Power System with Large Scale Wind Power Penetration

Hu, Weihao; Su, Chi; Chen, Zhe

*Published in:*

Proceedings of the 37th Annual Conference of the IEEE Industrial Electronics Society, IECON 2011

*DOI (link to publication from Publisher):*

[10.1109/IECON.2011.6119426](https://doi.org/10.1109/IECON.2011.6119426)

*Publication date:*

2011

*Document Version*

Early version, also known as pre-print

[Link to publication from Aalborg University](#)

*Citation for published version (APA):*

Hu, W., Su, C., & Chen, Z. (2011). Impact of Wind Shear and Tower Shadow Effects on Power System with Large Scale Wind Power Penetration. In *Proceedings of the 37th Annual Conference of the IEEE Industrial Electronics Society, IECON 2011* (pp. 878-883 ). IEEE Press. <https://doi.org/10.1109/IECON.2011.6119426>

### General rights

Copyright and moral rights for the publications made accessible in the public portal are retained by the authors and/or other copyright owners and it is a condition of accessing publications that users recognise and abide by the legal requirements associated with these rights.

- ? Users may download and print one copy of any publication from the public portal for the purpose of private study or research.
- ? You may not further distribute the material or use it for any profit-making activity or commercial gain
- ? You may freely distribute the URL identifying the publication in the public portal ?

### Take down policy

If you believe that this document breaches copyright please contact us at [vbn@aub.aau.dk](mailto:vbn@aub.aau.dk) providing details, and we will remove access to the work immediately and investigate your claim.

# Impact of Wind Shear and Tower Shadow Effects on Power System with Large Scale Wind Power Penetration

Weiha0 Hu, Chi Su, Zhe Chen  
Department of Energy Technology, Aalborg University, Denmark  
whu@et.aau.dk, csu@et.aau.dk, zch@et.aau.dk

**Abstract** – Grid connected wind turbines are fluctuating power sources due to wind speed variations, the wind shear and the tower shadow effects. The fluctuating power may be able to excite the power system oscillation at a frequency close to the natural oscillation frequency of a power system. This paper presents a simulation model of a variable speed wind farm with permanent magnet synchronous generators (PMSGs) and full-scale back-to-back converters in the simulation tool of DIgSILENT/PowerFactory. In this paper, the impacts of wind shear and tower shadow effects on the small signal stability of power systems with large scale wind power penetrations are investigated during continuous operation based on the wind turbine model and the power system model.

## I. INTRODUCTION

Because of energy shortage and environment pollution, the renewable energy, especially wind energy has attracted more attentions all over the world. It has been widely considered as one of the most rapidly increasing resource among other distributed generation technologies [1]. By 2020, it is expected that the total wind power generation will supply around 12% of the total world electricity demands [2].

As wind power rapidly develops recently, it's gradually taking a larger and larger part of the generation capacity. This could influence the topology and the power flow situation of the original power system especially when the integration of wind power increases to certain level. Consequently, the small signal stability of the power system will also be influenced, so it is necessary to investigate the small signal stability of power system with large scale wind power penetration [3].

Small signal stability is referred to as the ability of power systems to remain in synchronism under small disturbances [4], [5]. In today's interconnected power systems, small signal stability problem is often associated with the oscillatory stability problem which arises from lacking of sufficient damping torque [4], [5]. Several studies analyze the impact of fixed-speed wind turbines and variable-speed wind turbines on power system small signal stability [6-9]. The influence on the power system small signal stability of wind turbines based on fixed-speed induction generators, doubly fed induction generators (DFIGs) and permanent magnet synchronous generators (PMSGs) with full-scale back-to-back converters

are compared [6-9]. The study found that increasing the penetration of wind power generally had a positive effect, with increased damping of the inter-area mode oscillation between two interconnected power systems [9].

The wind power fluctuations produced by grid connected variable speed wind turbines during continuous operation is mainly caused by fluctuations in the aerodynamic torque due to wind speed variations, the wind shear and the tower shadow effects [10]. The wind shear and the tower shadow effects are normally referred to as the 3p oscillations. As a consequence, an output power drop will appear three times per revolution for a three bladed wind turbine. The frequency of the 3p oscillations is normally within the range associated with the local or inter-area mode oscillation frequency of a power system. So the 3p oscillations of wind power may be able to excite the power system oscillation at a frequency close to its natural oscillation frequency. In this paper, the impacts of wind shear and tower shadow effects on the small signal stability of power systems with large scale wind power penetrations are investigated during continuous operation.

Variable speed wind turbines with multipole permanent magnet synchronous generators and full-scale back-to-back converters are becoming more popular worldwide, because of some advantages such as no gearbox, high power density and easy to control [11]. In this paper, a variable speed wind turbine with a PMSG and a full-scale back-to-back converter is chosen as the study case. A simulation model of a variable speed wind farm with PMSGs and full-scale converters developed in DIgSILENT/PowerFactory is presented, and the control schemes of the wind turbine are described. Based on the wind turbine model and the power system model, the impacts of wind shear and tower shadow effects on the small signal stability of power systems with large scale wind power penetrations are investigated during continuous operation.

## II. WIND TURBINE MODEL AND CONTROL SCHEMES

### A. Wind Turbine Model

The wind turbine considered here applies a PMSG, using a back-to-back full-scale PWM voltage source converter connected to the grid. Variable speed operation of the wind turbine can be realized by appropriate adjustment of the rotor speed.

A complete wind turbine model includes the wind speed

model, the aerodynamic model of the wind turbine, the mechanical model of the drive train and models of the electrical components, namely the PMSG, PWM voltage source converters, transformer, and the control and supervisory system. Fig. 1 illustrates the main components of the grid connected wind turbine as well as the control schemes of the wind turbine.

Wind simulation plays an important task in the wind turbine modeling, particularly for dynamic interaction analysis between wind farms and the power system to which they are connected. A wind model which is applied in this paper has been developed [12]. The wind model provides an equivalent wind speed for each wind turbine, which is conveniently used as an input to a simplified aerodynamic model of the wind turbine.

A simplified aerodynamic model is normally used when the electrical behavior of the wind turbine is the main interest of the study. The relation between the wind speed and aerodynamic torque may be described by the following equation:

$$T_w = \frac{1}{2} \rho \pi R^3 v_{eq}^2 \frac{C_p(\theta, \lambda)}{\lambda} \quad (1)$$

where  $T_w$  is the aerodynamic torque extracted from the wind (Nm);  $\rho$  is the air density ( $\text{kg/m}^3$ );  $R$  is the wind turbine rotor radius (m);  $v_{eq}$  is the equivalent wind speed (m/s);  $\theta$  is the pitch angle of the rotor (deg),  $\lambda = \omega R / v_{eq}$  is the tip speed ratio;  $\omega$  is the wind turbine rotor speed (rad/s); and  $C_p$  is the aerodynamic efficiency of the rotor.

3p torque oscillations are important parts in the aerodynamic model. A comprehensive yet pragmatic model of 3p torque oscillations due to wind shear and tower shadow effects has been developed for a three-blade wind turbine [13], which is applied in this paper. Based on this model, the

equivalent wind speed ( $v_{eq}$ ) will have three components. The first ( $v_{eq_0}$ ) is the hub height wind speed, the second ( $v_{eq_{ws}}$ ) is due to the wind shear, and the third ( $v_{eq_{ts}}$ ) is due to the tower shadow. Therefore, the equivalent wind speed can be expressed as (2) whose components are shown as (3)-(5)

$$v_{eq} = v_{eq_0} + v_{eq_{ws}} + v_{eq_{ts}} \quad (2)$$

$$v_{eq_0} = V_H \quad (3)$$

$$v_{eq_{ws}} = V_H \left[ \frac{\alpha(\alpha-1)}{8} \left( \frac{R}{H} \right)^2 + \frac{\alpha(\alpha-1)(\alpha-2)}{60} \left( \frac{R}{H} \right)^3 \cos 3\beta \right] \quad (4)$$

$$v_{eq_{ts}} = \frac{mV_H}{3R^2} \sum_{b=1}^3 \left[ \frac{a^2}{\sin^2 \beta_b} \ln \left( \frac{R^2 \sin^2 \beta_b}{x^2} + 1 \right) - \frac{2a^2 R^2}{R^2 \sin^2 \beta_b + x^2} \right] \quad (5)$$

where  $V_H$  is the wind speed at hub height (m/s),  $\alpha$  is the empirical wind shear exponent,  $H$  is the elevation of rotor hub (m),  $\beta$  is the azimuthal angle of the blade (deg),  $\beta_b$  is respectively the azimuthal angle of each blade (deg),  $a$  is the tower radius (m),  $x$  is the distance from the blade origin to the tower midline (m), and  $m = \left[ 1 + \frac{\alpha(\alpha-1)R^2}{8H^2} \right]$  is a coefficient of the wind turbine.

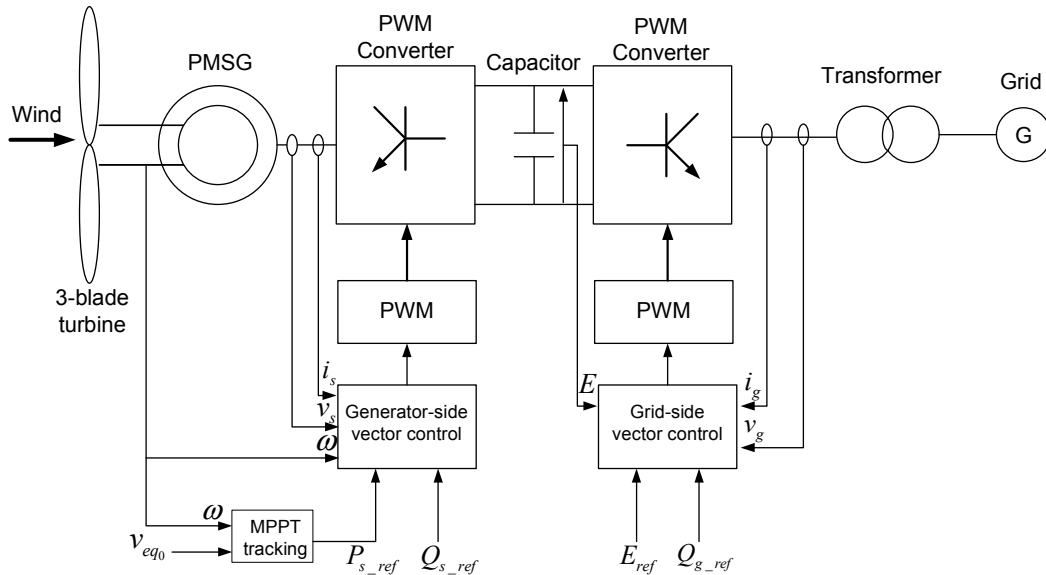


Fig. 1. Block diagram of a grid connected wind turbine with a PMSG and a full-scale converter.

As for the mechanical model, emphasis is put on the parts of the dynamic structure of the wind turbine that contribute to the interaction with the grid. Therefore, only the drive train is considered, while the other parts of the wind turbine structure, e.g. tower and flap bending modes, are neglected.

In this paper, the PMSG model with detailed description of the stator direct and quadrature axis currents, the magnetic strength and the rotor speed is applied, using generalized machine theory [14]. Since the study interest is not concentrated on the switches of the PWM converter, an average model without switches is used instead of the detailed PWM voltage source converter model so that the simulation can be carried out with a larger time step resulting in a simulation speed improvement [15].

### B. Control Schemes

For a variable speed wind turbine with a PMSG and a back-to-back full-scale converter, it is possible to control the electromagnetic torque at the generator directly, so that the speed of the turbine rotor can be varied within certain limits. An advantage of the variable speed wind turbine is that the rotor speed can be adjusted in proportion to the wind speed in low to moderate wind speeds so that the optimal tip speed ratio is maintained. At this tip speed ratio the aerodynamic efficiency,  $C_p$ , is at maximum, which means that the energy conversion is maximized. It is normally referred to as maximum power point tracking (MPPT) [16].

In general, variable speed wind turbines may have two different control goals, depending on the wind speed. In low to moderate wind speeds, the control goal is to maintain a constant optimum tip speed ratio for maximum aerodynamic efficiency. In high wind speeds, the control goal is to keep the rated output power fixed in order not to overload the system.

Vector control techniques have been well developed for PMSG using back-to-back PWM converters [17]. Two vector control schemes are designed respectively for the generator-side and grid-side PWM converters, as shown in Fig. 1.

The objective of the vector-control scheme for the grid-side PWM converter is to keep the DC-link voltage constant regardless of the magnitude of the generator power, while keeping sinusoidal grid currents. It may also be responsible for controlling reactive power flow between the grid and the grid-side converter by adjusting  $Q_{g\_ref}$ . The objective of the vector-control scheme for the generator-side PWM converter is to control the optimal power tracking for maximum energy capture from the wind by adjusting the speed of the wind turbine. The reference value of the generator active power  $P_{s\_ref}$  is obtained from the rotor speed controller. Normally, only the hub height wind speed  $v_{eq_0}$  in equation (2) could be measured by the wind speed sensor. The rotor speed reference is obtained via a look-up table to enable the optimal tip speed ratio. The rotor speed reference does not vary with the 3p oscillations from the wind shear and tower shadow effects.

Normally, the reference values of both generator-side and grid-side converters,  $Q_{s\_ref}$  and  $Q_{g\_ref}$  are set to zero to

ensure unity power factor operation and reduce currents of both generator-side and grid-side converters.

### III. SMALL SIGNAL STABILITY

Small signal stability is the ability of a power system to maintain synchronism among generators under small disturbances. It is the nature of a power system at a certain operating point [18].

A power system can be described by a state equation in the form of (6) (with the assumption of zero input).

$$\frac{dX}{dt} = f(X) \quad (6)$$

In (6),  $X$  denotes the state vector of the power system,  $t$  denotes the time and  $f$  is normally a set of nonlinear functions.

To analyze the small signal stability of the power system at an operating point, the first step is to linearize the state equation at this operating point by Taylor's series expansion. The linearized state equation is in the form of (7).

$$\frac{d\Delta X}{dt} = A \cdot \Delta X \quad (7)$$

In (7), the prefix  $\Delta$  denotes a small deviation and  $A$  is the state matrix. The small signal stability is given by the eigenvalues of matrix  $A$ . Eigenvalues are in the form of (8).

$$\lambda = \sigma \pm j \cdot \omega \quad (8)$$

Each eigenvalue (or a conjugate pair) corresponds to an oscillation mode of the power system at the analyzed operating point. The real component of an eigenvalue  $\sigma$  gives the damping and the imaginary component  $\omega$  gives the frequency of the corresponding mode. The small signal stability is then determined as follows:

- when all eigenvalues have negative real parts, the system is stable;
- when at least one eigenvalue has positive real part, the system is unstable;
- when at least one eigenvalue has zero real part, the stability of the system can not be told in this way.

The information of the decay rate of the oscillation can be also drawn from eigenvalues by a variable termed as damping ratio which is in the form of (9).

$$\zeta = \frac{-\sigma}{\sqrt{\sigma^2 + \omega^2}} \quad (9)$$

This is a common index of small signal stability analysis. The larger  $\zeta$  is, the system is considered to have wider stability margin.

The frequency of the wind power 3p oscillations due to the wind shear and tower shadow effects is normally within the range associated with the local or inter-area mode oscillation frequency of a power system. The 3p oscillations of wind power may be able to excite the power system oscillation at a

frequency close to its natural oscillation frequency  $\omega$  in (8). In this paper, the impacts of wind shear and tower shadow effects on the small signal stability of power systems with large scale wind power penetrations are investigated during continuous operation.

#### IV. CASE STUDY

A two area test power system with large scale wind power integration is selected and shown in Fig. 2. The test power system is often used to study the fundamental nature of inter-area oscillations [19]. The 12 bus test power system consists of four synchronous generators, two loads, and an aggregated wind farm. Area 1 has two synchronous generators, each with a capacity of 380 MVA and Area 2 also has two synchronous generators, each also with a capacity of 380 MVA. All four synchronous generators are identical. A wind farm based on PMSG and a full-scale back-to-back converter is connected to the grid in Area 1. The maximum output of the wind farm is assumed to be 500 MW, which supports 33% loads in the studied power system. The aggregated wind farm is modeled using a PMSG and a full-scale back-to-back converter as described in Section II. It is assumed in this paper that all the wind turbines in the wind farm rotate at the same speed and in the same phase.

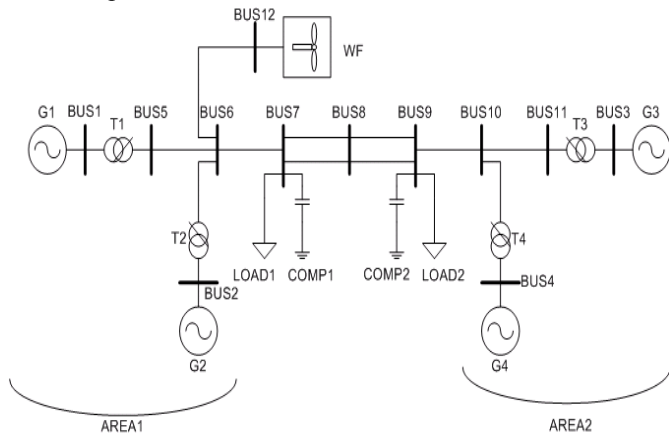


Fig. 2. The two area test power system with large scale wind power integration.

Table I summarizes the oscillation modes of the test power system without wind power penetrations. There are three oscillation modes in the power system, two intra-area oscillation modes (mode 1 and mode 2) and one inter-area oscillation mode (mode 3). It can be seen that the dominant dynamic behavior of the power system is an inter-area oscillation mode between the G1, G2 in the Area 1 and the G3, G4 in the Area 2. So the following investigations focus on the inter-area oscillation mode.

TABLE I  
THE OSCILLATION MODES OF THE POWER SYSTEM

Oscillation Mode	Eigenvalue	Frequency (Hz)	Damping Ratio (%)
Mode 1	$-0.935 \pm j6.22$	0.99	14.9
Mode 2	$-0.906 \pm j6.47$	1.03	13.9
Mode 3	$-0.192 \pm j3.96$	0.63	4.84

Fig. 3 illustrates the variation of the inter-area oscillation damping ratio with the wind speed. The inter-area oscillation damping ratio increases when the wind speed increases. It implies that the power system is more stable when there are larger wind power penetrations in the power system. Fig. 4 shows the variation of the inter-area natural oscillation frequency and the wind turbine 3p frequency due to the wind shear and tower shadow effects with the wind speed. It can be seen that the inter-area natural oscillation frequency decreases slightly when the wind speed increases. However, the wind turbine 3p frequency due to the wind shear and tower shadow effects increases when the wind speed increases. The 3p frequency equals to the inter-area natural oscillation frequency at a certain value of wind speed, which is around 8 m/s in this case.

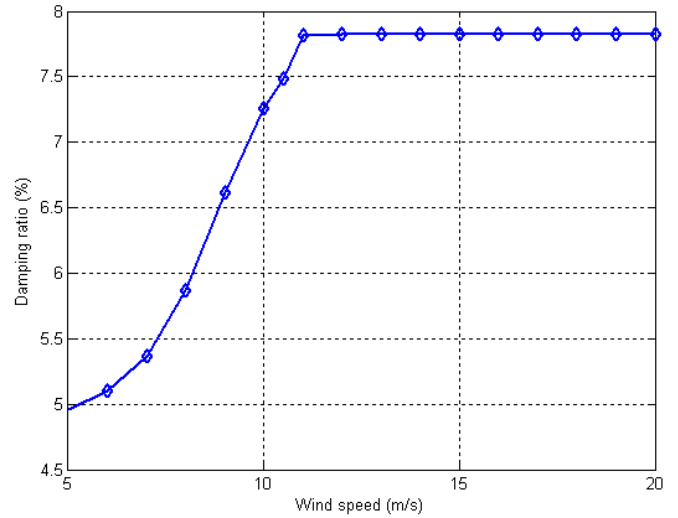


Fig. 3. The variation of the inter-area oscillation damping ratio with the wind speed.

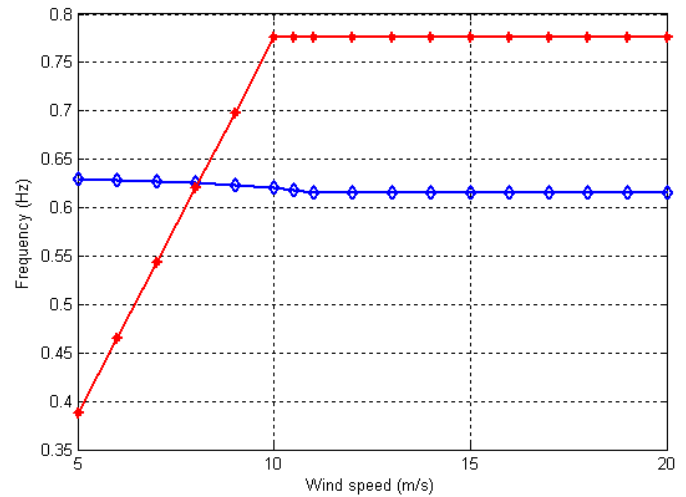


Fig. 4. The variation of the inter-area natural oscillation frequency (blue diamond) and the wind turbine 3p frequency (red asterisk) with the wind speed.

Figs. 5-7 illustrate the equivalent wind speed, the wind power, the active power of generator 1, the active power of generator 3 and the active power of the transmission line between bus 7 and bus 9 during different wind speed periods.

In the low wind speed period ( $v = 5$  m/s), the power oscillations caused by the wind shear and tower shadow effects of the wind farm are small in the active power of generator 1, generator 3 and the transmission line, even though the inter-area oscillation damping ratio is very small. The inter-area oscillation damping ratio increases when the wind speed increases, which implies that the power system is more stable. However, in the medium wind speed period ( $v = 8$  m/s), the power oscillations caused by the wind shear and tower shadow effects of the wind farm are much larger in the active power of generator 1, generator 3 and the transmission line, because the 3p oscillations of wind power excite the power system inter-area natural oscillation in the medium wind speed period. In the high wind speed period ( $v = 15$  m/s), the power system oscillations are relatively small, since the input 3p oscillation frequency of wind power is far away from the inter-area natural oscillation frequency.

The wind power oscillations and the active power oscillations in the transmission line between bus 7 and bus 9 with the wind speed is shown in Fig. 8. It can be seen that wind power oscillations due to the wind shear and tower shadow effects increase with the wind speed. However, the power oscillations in the transmission line in the medium wind speed period ( $v = 8$  m/s) are larger than the power oscillations in other wind speed periods.

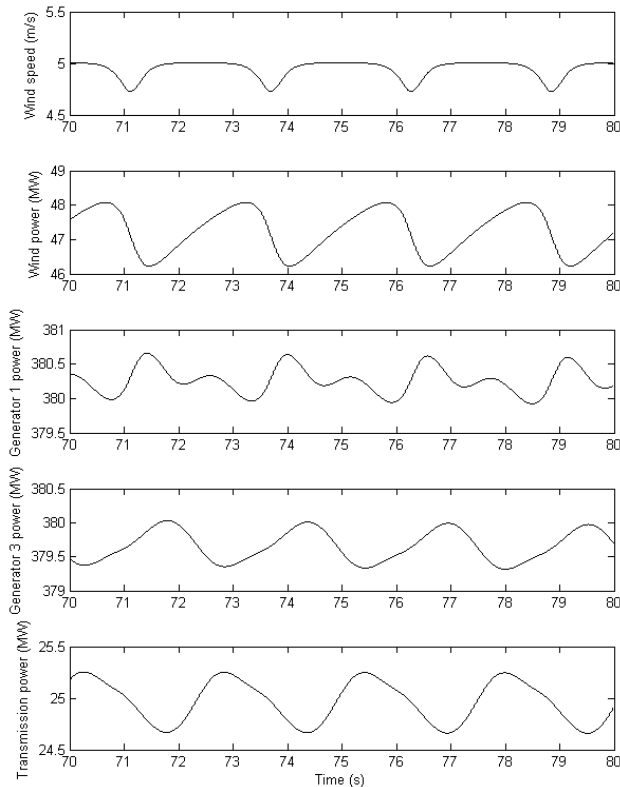


Fig. 5. The equivalent wind speed, the wind power, the active power of generator 1, the active power of generator 3 and the active power of the transmission line between bus 7 and bus 9 during the low wind speed period ( $v = 5$  m/s).

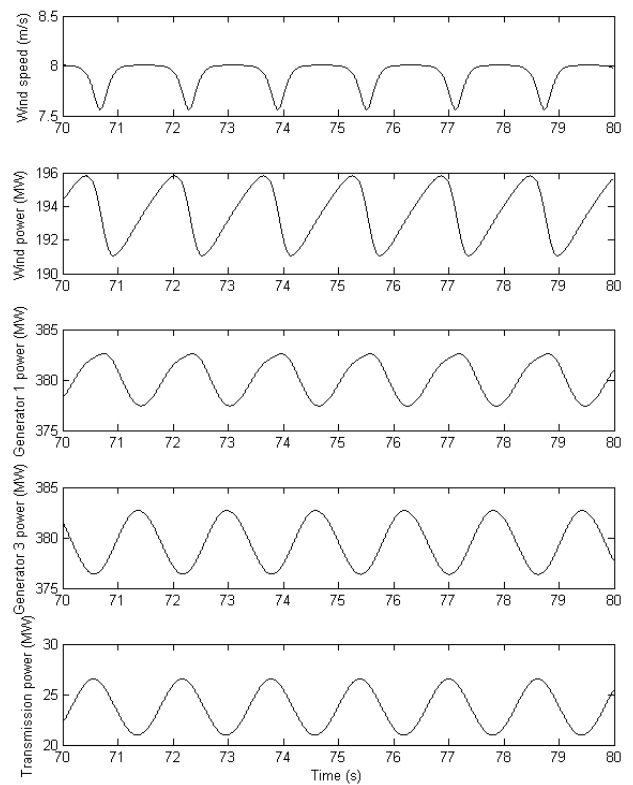


Fig. 6. The equivalent wind speed, the wind power, the active power of generator 1, the active power of generator 3 and the active power of the transmission line between bus 7 and bus 9 during the medium wind speed period ( $v = 8$  m/s).

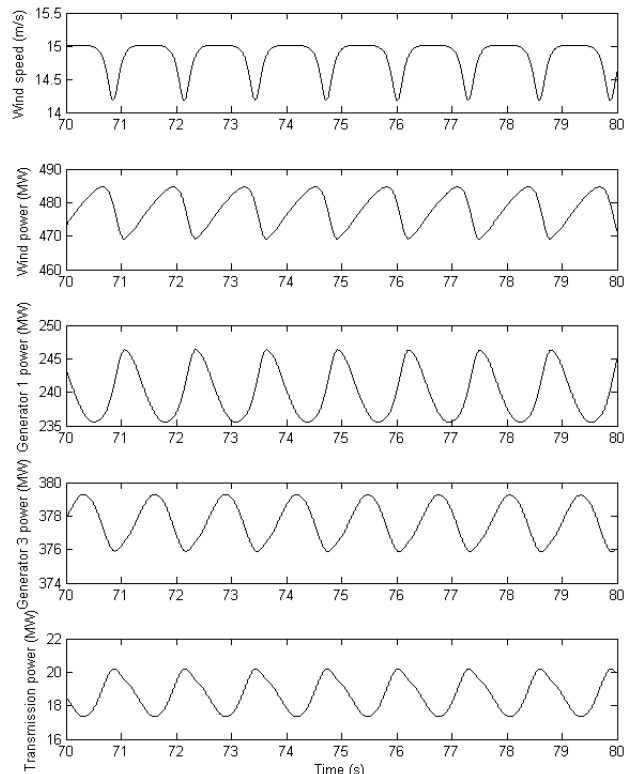


Fig. 7. The equivalent wind speed, the wind power, the active power of generator 1, the active power of generator 3 and the active power of the transmission line between bus 7 and bus 9 during the high wind speed period ( $v = 15$  m/s).

The amplifying factor ( $AF$ ) between the transmission power oscillations ( $\Delta P_{line}$ ) and wind power oscillations ( $\Delta P_{wind}$ ) due to the wind shear and tower shadow effects could be defined as

$$AF = \frac{\Delta P_{line}}{\Delta P_{wind}} \quad (10)$$

Fig. 9 illustrates the amplifying factor between the transmission power oscillations and wind power oscillations with the wind speed. It can be seen that amplifying factor are larger in medium wind speed periods and lower in both low and high wind speed periods, because the 3p oscillation frequency due to the wind shear and tower shadow effects is close to the inter-area natural oscillation frequency of the power system in medium wind speed periods even though the damping ratio is relatively high compared with the damping ratio in low wind speed periods.

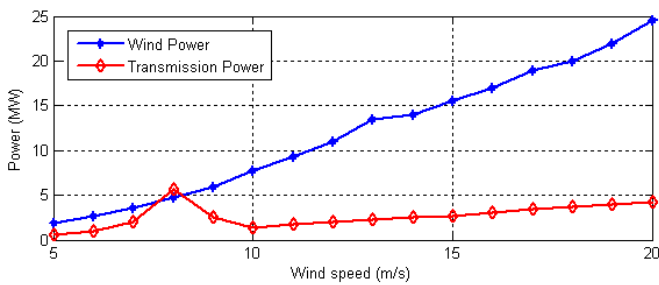


Fig. 8. The wind power oscillations and the active power oscillations in the transmission line between bus 7 and bus 9 with the wind speed.

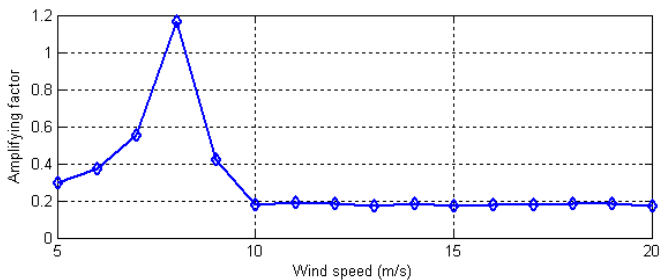


Fig. 9. The amplifying factor between the transmission power oscillations and wind power oscillations with the wind speed.

## V. CONCLUSION

In this paper, the model of variable speed wind turbines with permanent magnet synchronous generators using the full-scale back-to-back PWM voltage source converters and the corresponding control schemes are developed in the simulation tool of DIGSILENT/PowerFactory. On the basis of the developed wind turbine model and power system model, the small signal stability of power systems with large scale wind power penetrations are investigated. The inter-area oscillation damping ratio of the 12 bus test power system increases when there are larger wind power penetrations in the power system, which implies that the power system is more stable. It can be concluded from the simulation results that power system oscillations due to the wind shear and tower shadow effects are larger in medium wind speed

periods, because 3p oscillation frequency of the studied wind turbines is close to the inter-area natural oscillation frequency of the test power system in medium wind speed periods.

## REFERENCES

- [1] S. Heier, *Grid integration of wind energy conversion systems*. Chichester, U.K. Wiley, 2006.
- [2] The European Wind Energy Association (EWEA), *Wind force 12*. Oct. 2002. [Online]. Available: <http://www.ewea.org/doc/WindForce12.pdf>
- [3] C. Su, Z. Chen, "An optimal power flow (OPF) method with improved power system stability," *IEEE International Universities Power Engineering Conference (UPEC)*, pp. 1-6, 2010.
- [4] P. Kundur, J. Paserba, V. Aiarapu et al., "Definition and classification of power system stability," *IEEE Trans. Power Syst.*, vol. 19, no. 3, pp. 1387-1401, 2004.
- [5] W. Du, H.F. Wang and R. Dunn, "Power system oscillation stability and control by facts and ESS-survey", *International Conference on Sustainable Power Generation and Supply*, pp. 1-13, 2009.
- [6] O. Anaya-Lara, F. Hughes, N. Jenkins, and G. Strbac, "Influence of windfarms on power system dynamic and transient stability," *Wind Engineering*, vol. 30, no. 2, pp. 107-27, 2006.
- [7] E. Hagstrom, I. Norheim, and K. Uhlen, "Large-scale wind power integration in Norway and impact on damping in the Nordic grid," *Wind Energy*, vol. 8, no. 3, pp. 375-384, Jul.-Sep. 2005.
- [8] J. Slootweg and W. Kling, "The impact of large scale wind power generation on power system oscillations," *Electric Power Systems Research*, vol. 67, no. 1, pp. 9-20, 2003.
- [9] T. Knüppel, V. Akhmatov, J. N. Nielsen, K. H. Jensen, A. Dixon, J. Østergaard, "Small-Signal Stability Analysis of Full-Load Converter Interfaced Wind Turbines," *International Workshop on Large-Scale Integration of Wind Power into Power Systems as well as on Transmission Networks for Offshore Wind Farms*, pp. 1-8, 2009.
- [10] Å. Larsson, "Flicker emission of wind turbines during continuous operation," *IEEE Trans. Energy Convers.*, vol. 17, no. 1, pp. 114-118, Mar. 2002.
- [11] M. Chinchilla, S. Arnaltes, and J. C. Burgos, "Control of permanent-magnet generators applied to variable-speed wind-energy systems connected to the grid," *IEEE Trans. Energy Convers.*, vol. 21, no. 1, pp. 130-135, May. 2006.
- [12] P. A. C. Rosas, P. Sørensen, and H. Bindner, "Fast wind modeling for wind turbines," in *Proc. Wind Power 21st Century EUWER Special Topic Conf. Exhibit.*, Kassel, Germany, Sep. 2000, pp. 184-187.
- [13] D. S. L. Dolan, and P. W. Lehn, "Simulation model of wind turbine 3p torque oscillations due to wind shear and tower shadow," *IEEE Trans. Energy Convers.*, vol. 21, no. 3, pp. 717-724, Sep. 2006.
- [14] I. M. Canay, "Causes of discrepancies on calculation of rotor quantities and exact equivalent diagrams of the synchronous machine," *IEEE Trans. Power Apparatus and Systems*, vol. 88, no. 7, pp. 1114-1120, Jul. 1969.
- [15] P. Giroux, G. Sybille, and H. Le-Huy, "Modeling and simulation of a distribution STATCOM using Simulink's power system blockset," in *Proc. 27th Annual Conf. IEEE Industrial Electronics Society*, Denver, USA, Nov. 2001, pp. 990-994.
- [16] G.D. Moor, and H.J. Beukes, "Maximum power point trackers for wind turbines," in *Proc. of 35th Annual IEEE Power Electronics Specialists Conference*, Aachen, Germany, Jun. 2004, pp. 2044-2049.
- [17] T. Senjyu, T. Shimabukuro, and K. Uezato, "Vector control of permanent magnet synchronous motors without position and speed sensors," in *Proc. of 26th Annual IEEE Power Electronics Specialists Conference*, Atlanta, USA, Jun. 1995, pp. 759-765.
- [18] P. Kundur, *Power System Stability and Control*. New York: McGraw-Hill, 1994.
- [19] M. Klein, G. J. Rogers, and P. Kundur, "A fundamental study of inter-area oscillations in power systems," *IEEE Transactions on Power Systems*, vol. 6, pp. 914-921, 1991.